Journal of Applied Polymer Science

Synthesis and Characterization of Poly(hydroxylic fluoroacrylate)/$mSiO_2$ Nanocomposite by *In Situ* Solution Polymerization

Hu Liu, Baosong Fu, Qianqian Shang, Guomin Xiao
School of Chemistry and Chemical Engineering, Southeast University, Nanjing 211189, People's Republic of China

Correspondence to: G. Xiao (E-mail: xiaogm@seu.edu.cn)

ABSTRACT: In this study, vinyl-group modified nanosilicas ($mSiO_2$) were prepared via sol–gel method using vinyltriethoxysilane (VTES) as modifier first, then the novel poly(hydroxylic fluoroacrylate)/$mSiO_2$ nanocomposite was successfully synthesized by *in situ* solution polymerization of $mSiO_2$ with dodecafluoroheptyl methacrylate (DFHMA), β-hydroxyethyl methacrylate (HEMA), methyl methacrylate (MMA), and butyl acrylate (BA) initiated by 2,2-azobisisobutyronitrile (AIBN) in the co-solvents of ethyl acetate and butyl acetate. The chemical composition and structure of the nanocomposite were characterized by Fourier transform infrared spectrometry (FTIR) and transmission electron microscopy (TEM). TEM observation indicated that $mSiO_2$ nanoparticles obtained a well dispersion in polymeric matrix. Thermogravimetric analysis (TGA) studies revealed that the temperature corresponding to 50% weight loss of the nanocomposite was improved by 21.5°C with the addition of 2.0 wt % $mSiO_2$. The synthesized nanocomposites were applied to use with hexamethylene diisocyanate trimer (HDIT) to prepare polyurethane materials. Tensile test revealed that polyurethane material with $mSiO_2$ content of 2.0 wt % showed an ultimate tensile strength of about 5.19 times higher than that without $mSiO_2$. The polyurethane films displayed surface energy of lower than 25 mN m^{-1} and high light transmittance. © 2012 Wiley Periodicals, Inc. J. Appl. Polym. Sci. 000: 000–000, 2012

KEYWORDS: nanocomposites; fluoropolymers; VTES-modified SiO_2; *in situ* solution polymerization; polyurethane

Received 23 May 2011; accepted 18 March 2012; published online
DOI: 10.1002/app.37739

INTRODUCTION

Organic–inorganic nanocomposites have drawn much attention in both fundamental research and practical applications during the past decade.[1–3] The combination of organic polymer and inorganic nanoparticles would endow the hybrid materials with improved performances such as mechanical strength, hardness, thermal stability, and corrosion resistance, and so on.[4–6] Nanosilica is an important member in the family of inorganic materials and there have been many published work concerning the preparation of nanocomposites with nanosilica. For example, Hong et al. have successfully employed silica nanoparticles into polymethylmethacrylate (PMMA) by *in situ* bulk polymerization, and the resultant hybrids showed higher glass transition temperature, surface hardness, and impact strength than pure PMMA.[7] Zheng et al. have prepared PMMA/SiO_2 nanocomposites with improved thermal properties via *in situ* suspension polymerization.[8] The improved performances of the reported nanocomposites were obtained only when the nanoparticles get well dispersion in polymeric matrix.[9] However, due to the enormous specific surface area and high surface energy of nanosilicas, the particles are prone to aggregation. Besides, the surface of pure nanosilicas is hydrophilic, which is incompatible with hydrophobic polymeric matrix. Therefore, it is indispensable to modify nanosilicas to render each nano-individual stable and not to agglomerate. Generally, γ-methacryloxypropyl trimethoxy silane (MPS), a kind of silane coupling agents, was used as the modifier to graft double bonds on the surface of nanosilicas.[10–12] The modification process, though widely used, was preceded in organic solvent of toluene or xylene and, moreover, the grafting amount was relative low and the modification result was not very ideal, which was reflected by lipophilic degree.[7] Here we chose vinyltriethoxysilane (VTES) as the modifier to prepare vinyl group functionalized nanosilicas via sol–gel process to improve the lipophilic degree. In contrast with the method mentioned above, the processes of preparation and modification nanosilicas occurred simultaneously.

Fluorinated polymers are known for their desirable properties including high thermal and chemical stability; low surface energy, dielectric constants, and flammability; excellent mechanical features and corrosion resistance.[13–15] Among the

fluoropolymers, fluoroacrylate polymers are widely used with an increasing trend in the areas of construction, automotive, navigation, and aerospace industries.[16,17] While most of the reported fluoroacrylate polymers were prepared via various emulsion polymerization techniques.[18–22] The disadvantage of these techniques is that the constituent of the emulsion is complex and the residual emulsifiers in the resin are hard to remove. So the hydrophobicity of the film is partially offset by the residual hydrophilic emulsifiers. Zhang et al. have revealed out that the water and oil repellency of the latex film is inferior to solvent-borne film.[23] In addition, as revealed in Chen et al. study, *in situ* polymerization method was superior to traditional blending method in terms of the dispersion of nanoparticles in polymeric matrix. They reported that basically homogeneous nanosilica particles appeared in polyester polyol/nanosilica composite resins prepared by *in situ* polymerization whereas some aggregation occurred in polyester polyol/nanosilica composite resins prepared by the blending method.[24] The objective of this research is to prepare nanocomposites with the merits of organic fluoropolymer and inorganic nanosilicas through the technique of *in situ* solution polymerization. Dodecafluoroheptyl methacrylate (DFHMA) and hydroxyethyl methacrylate (HEMA) were adopted as fluorine-containing monomer and hydroxyl-containing monomer, respectively. Vinyl group functionalized nanosilicas were prepared and different amounts of them were introduced into the polymerization. And also, the tensile properties, thermal stability, light transmittance, and surface properties of the nanocomposites were investigated.

EXPERIMENTAL

Materials and Apparatus

Tetraethylorthosilicate (TEOS) (A.R.), absolute ethanol (A.R.), and ammonia (25 wt % in water), were purchased from Sinopharm Chemical Reagent (China). Vinyltriethoxysilane (VTES) (Shanghai Silicon Mountain Macromolecular Materials, China) and β-hydroxyethyl methacrylate (HEMA) (Aladdin-reagent, Shanghai, China) were used as received. Hexamethylene diisocyanate trimer (HDIT), with the trade mark of Desmodur N3600 (NCO% = 23.0 ± 0.5%), was supplied by Bayer Company (Germany). Dodecafluoroheptyl methacrylate (DFHMA), with the molecular formula of CH_2=$CHCOOCH_2CF(CF_3)CFHCF(CF_3)_2$, was obtained from XEOGIA Fluorine-Silicon Chemical (China) and used after distillation under vacuum. MMA and BA, purchased from LingFeng Chemical Regent, (China), were first washed by 10 wt % aqueous solution of sodium hydroxide to remove inhibitor, and then by distilled water thoroughly. The washing-treated monomers were dried over anhydrous magnesium sulfate for 48 h followed by distillation under vacuum before use. Azobisisobutyronitrile (AIBN) was used after recrystallization in ethanol. The solvents of ethyl acetate (EA) and butyl acetate (BAT) are analytical grade. Ultrasonication through the experiment was performed in a KH5200B ultrasonic cleaner with the frequency of 40 KHz and power of 200 W (KunShan HeChuang Ultrasonic, China). The ultrasonic medium (water) was recirculated and cooled to keep the temperature at the range of 16–18°C during ultrasonication process.

Preparation of Vinyl-Group Modified Nanosilicas ($mSiO_2$)

Nanosilicas were synthesized by the modified Stober method as follows[25]: In a 250-mL four-necked round-bottomed flask equipped with a magnetic stirrer and a dropping funnel, 80.0 mL ethanol, 5.0 mL ammonia, and 3.0 mL deionized water were mixed and magnetically stirred at 300 rpm for 1 h at a constant temperature of 50°C. Afterward, a solution of 25.0 mL TEOS, 5.0 mL VTES, and 20.0 mL ethanol was dropwise added into the flask. The mixture was allowed to react for 12 h isothermally at 50°C to form gelatin, then transferred into a hydrothermal reaction vessel and aged at 120°C for 24 h. After filtration, rinsing with ethanol and drying under vacuum at 40°C for 12 h sequentially, the hydrophobic nanosilica powders were obtained.

In Situ Solution Polymerization of Poly(Hydroxylic Fluoroacrylate)/$mSiO_2$ Nanocomposites (PHFA/$mSiO_2$)

PHFA/$mSiO_2$ nanocomposites were prepared by *in situ* solution polymerization. A typical synthetic process was employed as follows: the monomers of MMA (8.0 g), BA (13.0 g), DFHMA (4.5 g), and HEMA (4.5 g) as well as initiator (AIBN, 0.6 g) were dissolved in the mixed solvents of EA (10 mL) and BAT (20 mL), and then $mSiO_2$ (0.6 g) was added in the solution followed by ultrasonic treatment for 0.5 h until obtaining a milky-white suspension system. In a 250-mL four-necked flask, equipped with mechanical stirrer, reflux condenser, dropping funnel, and gas inlet cock, EA (10 mL) and BAT (20 mL) were heated at 85°C for 5 min under nitrogen atmosphere. Then the prepared mixture was dropwise added into the flask within 1–1.5 h. The reaction mixture was stirred isothermally at 85°C for another 4 h to achieve a higher conversion. Upon cooling at room temperature, PHFA/$mSiO_2$ nanocomposite solution with 2.0 wt % of $mSiO_2$ was obtained. Pure PHFA polymer was also synthesized under the similar procedure as PHFA/$mSiO_2$ nanocomposites just without $mSiO_2$. The final monomer conversions were calculated by gravimetric analysis according to the following formulas:

$$C(\%) = \frac{S \times W_p - W_i - W_{\mathrm{mSiO2}}}{W_m} \times 100 \qquad (1)$$

where W_m is the weight of total monomers, W_p is the weight of product solution, S is the solid content of the product solution, W_i and W_{mSiO2} are the weights of initiator and $mSiO_2$ put into the flask, respectively. The detailed recipes and conversions of the prepared samples are listed in Table I.

Preparation of Polyurethane Materials

In practice, hydroxylic polyacrylate resin is commonly used in conjunction with crosslink agent, such as polyisocyanate, to prepare polyurethane materials. Herein, we took sample 4 as an example of preparing polyurethane material. 43.5 g of PHFA/$mSiO_2$ nanocomposite solution was mixed with 5 g of component solvent (EA, BAT, and acetone with a volume ratio of 3 : 3 : 1) at 300 rpm for 10 min, and then HDIT (Caution! Wear protective gloves, safety goggles, and mask when handling HDIT), a widely used curing agent, was added with the NCO/OH molar ratio of 1.1 followed by stirring at around 500 rpm for 20 min. The NCO/OH molar ratio of 1.1 was also selected

Table I. Recipes for Preparation of PHFA/$mSiO_2$ Nanocomposites

Sample	$mSiO_2$ (g)	Monomers (g)				Solvents (mL)		Initiator (g)	Conversion (%)
		MMA	BA	DFHMA	HEMA	EA	BAT	AIBN	
1	0	8.0	13.0	4.5	4.5	20	40	0.6	99.75
2	0.15	8.0	13.0	4.5	4.5	20	40	0.6	99.03
3	0.3	8.0	13.0	4.5	4.5	20	40	0.6	99.34
4	0.6	8.0	13.0	4.5	4.5	20	40	0.6	99.51

for other samples. The mixture was ultrasonicated for 15 min to remove air bubbles. For tensile testing, the prepared mixture was poured into a mould with a size of 14 cm × 4 cm × 1 cm. The mold was placed into an oven to evaporate the solvents at 35°C for 10 h and cure the mixture at 80°C for 2 h, and then the membrane was produced with the thickness of about 2 mm. For transparency and contact angle measurements, the prepared mixture was coated on a slide and cured at 80°C to form the film with the thickness of about 20 μm. Pure polyurethane was also processed under the similar conditions like sample 4.

Characterization

As the synthesized PHFA/$mSiO_2$ nanocomposites cannot dissolve in *n*-hexane, when the prepared nanocomposite solutions were added into *n*-hexane, PHFA/$mSiO_2$ nanocomposites can be precipitated from the solvents. After filtering, PHFA/$mSiO_2$ nanocomposites were dried under vacuum at 25°C for 24 h to remove the *n*-hexane. FTIR spectra of PHFA/$mSiO_2$ and $mSiO_2$ were recorded in transmission mode with KBr wafer on a Nicolet 5700 spectrometer.

TEM observations were carried out using a JEOL JEM-2000EX instrument with an accelerating voltage of 120 kV. One drop of PHFA/$mSiO_2$ nanocomposite solution (sample 4) was deposited in a copper mesh grid and evaporated solvents before observation. TEM image of dispersion state of $mSiO_2$ before *in situ* solution polymerization was obtained as follows: 0.1 g of $mSiO_2$ was dispersed in 15 mL butyl acetate following ultrasonic treatment for 0.5 h, and then observation was ready by depositing one drop of this dispersion on a copper mesh and evaporating butyl acetate. For determination of particle size distribution about 300 particles from random regions of a sample were measured manually using the software Image J.

Thermogravimetric analysis (TGA) of PHFA/$mSiO_2$ nanocomposites was performed on a SDT Q600 instrument. About 40–60 mg samples were measured over the temperature range of 50–700°C at a heating rate of 20°C min^{-1} under nitrogen atmosphere. Each sample was measured twice and the average value was taken.

Tensile tests of the prepared polyurethane membranes were determined on an Electronic Universal Testing Machine (WDW-20, Kexin Instruments, Changchun, China) at the load weight of 20 kN and a crosshead rate of 5 mm min^{-1}. The tensile specimens were dumb-bell-shaped, and the dimensions were determined with reference to national standard GB/T 528-2009 Type 1. All the tests were carried out at 25°C and 50% relative humidity. The ultimate tensile strength (UTS) was calculated by dividing the maximum load on a material experienced during a tensile test by the initial cross-section of the test sample. Strain at break (εB), also known as fracture strain, was the ratio between changed length and initial length after breakage of the test specimen. Young's modulus (E) was defined as the ratio of the uniaxial stress over the uniaxial strain in the range of stress in which Hooke's Law holds. The data of UTS, εB, and E reported herein were the average of five measurements. One-way analysis of variance (ANOVA) was used to determine statistical significance of differences between means in each group. The level of significance was $P < 0.05$.

The cross-section surfaces of the samples after tensile tests were observed by a scanning electron microscope (SEM) (JEOL, JSM-6360LV) with an accelerating voltage of 20 kV, after putting the specimens on a SEM disk and sputter-coated with gold layer to reduce charge buildup effects by electrons.

The contact angles of water and glycol on the polyurethane films were measured based on sessile drop method using a contact angle meter (JC2000C1 of ZhongChen Digital Technical Apparatus, China), and the reported results were the averages of five measurements. The surface energies of the prepared films can be calculated by the following equation:[26,27]

$$\gamma_s = \gamma_s^d + \gamma_s^p \tag{2}$$

$$\gamma_l(\cos\theta + 1) = 2(\gamma_s^d \gamma_l^d)^{1/2} + 2(\gamma_s^p \gamma_l^p)^{1/2} \tag{3}$$

where γ_s represents the surface energy of the film, γ_s^d and γ_s^p represent dispersion and polar items of the surface energy, respectively. The two testing liquids are deionized water and ethylene glycol, wherein, γ_l, γ_l^d and γ_l^p of deionized water are 72.8, 21.8, and 51.0 mN m^{-1} and of ethylene glycol are 48.3, 29.3, and 19 mN m^{-1}.[28]

UV–vis transmission spectra of the polyurethane films were obtained with a Shimadzu 2450 UV–vis spectrometer.

RESULTS AND DISCUSSION

FTIR Characterization

FTIR spectra of the pure and modified nanosilicas were shown in Figure 1(a,b). Both spectra showed characteristic absorption of SiO_2 at 1087 cm^{-1} (Si—O asymmetric stretching) and 472 cm^{-1} (Si—O—Si bending vibration).[29] For the spectrum of pure SiO_2 (spectrum a), a distinct absorption peak at 1645 cm^{-1} was assigned to the bending mode of physically absorbed water molecules. The broad band at 3440 cm^{-1} was attributed to hydroxyl group on the surface of silica. While for the spectrum of $mSiO_2$ (spectrum b), the absorption peak at 3440 cm^{-1} was weaker and another two characteristic absorption of C=C group at 1601

Applied Polymer SCIENCE

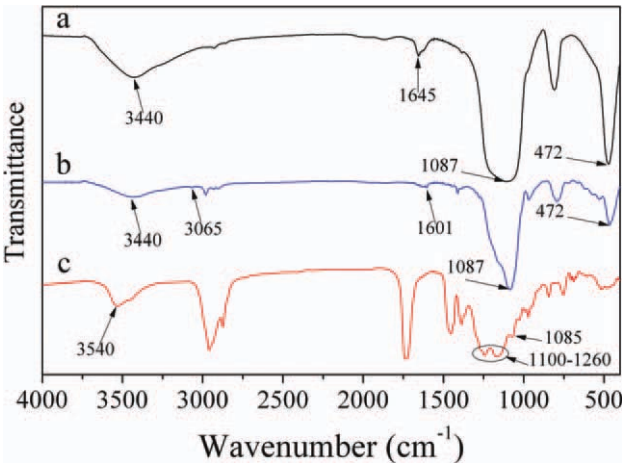

Figure 1. FTIR spectra of (a) pure SiO_2, (b) $mSiO_2$, (c) PHFA/$mSiO_2$ nanocomposite (mSiO2 1.0 wt %). [Color figure can be viewed in the online issue, which is available at wileyonlinelibrary.com.]

and 3065 cm^{-1} were detected, which indicated the lost of hydroxyl groups and the grafting of C=C groups on the surface of $mSiO_2$. Figure 1(c) showed the FTIR spectrum of PHFA/$mSiO_2$ nanocomposites with $mSiO_2$ content of 1.0 wt %. No absorption was observed at 1600–1640 cm^{-1} characteristic for the C=C bonds, indicating that monomers were polymerized. The wide and broad absorption band at 1100–1260 cm^{-1} was the overlap of the stretching vibration absorption of C—F group at 1100–1240 cm^{-1} and the stretching vibration absorption of C—O—C group at 1245 cm^{-1}.[30] Characteristic absorption of SiO_2 was detected at 1085 cm^{-1}, indicating that nanosilicas were embedded in polymeric matrix. The absorption at 3540 cm^{-1} was ascribed to the stretching vibration of hydroxyl group derived from HEMA.

Modification Mechanism of $mSiO_2$

The modification mechanism was presented in Figure 2. In alkaline environment, TEOS and VTES were hydrolyzed with water to bring out silanol groups. Hydroxyl condensation afterward occurred between these silanol groups, and then the vinyl groups modified nanosilicas formed. It was worth mentioning in this work that the processes of preparation and modification nanosilicas occurred simultaneously. Generally, the hydrophobicity of the modified SiO_2 can be quantified by the so-called lipophilic degree (LD), which was measured by dispersing of 0.5 g $mSiO_2$ in 50 mL water with the addition of methanol. The VTES-modified SiO_2 was hydrophobic and floated on the water. After adding methanol into the water slowly and stirring con-

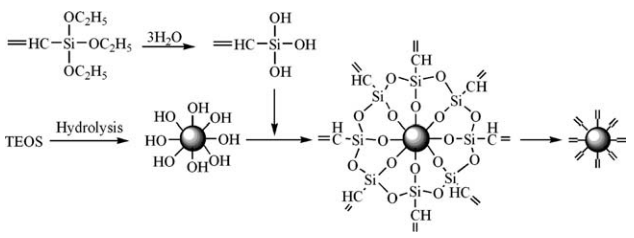

Figure 2. Modification mechanism of VTES modified SiO_2.

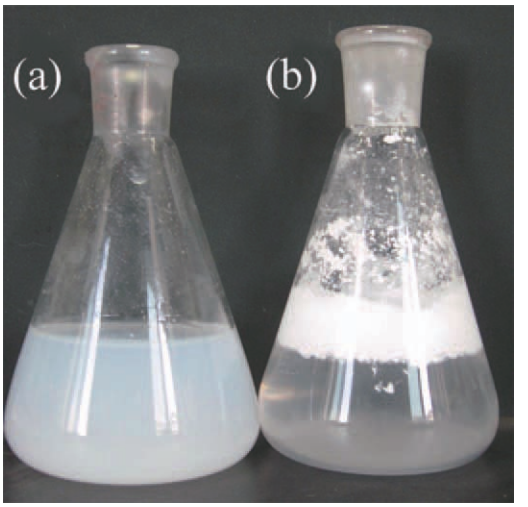

Figure 3. Hydrophobicity of pure SiO_2 (a) and $mSiO_2$ (b).

tinuously, $mSiO_2$ nanoparticles were wetted and precipitated gradually. The LD was calculated by the following equation:[31]

$$\mathrm{LD} = \frac{V}{V + 50} \tag{4}$$

where V (mL) was the volume of the used methanol. The LD of $mSiO_2$ in this research was 10.1%, which was higher than

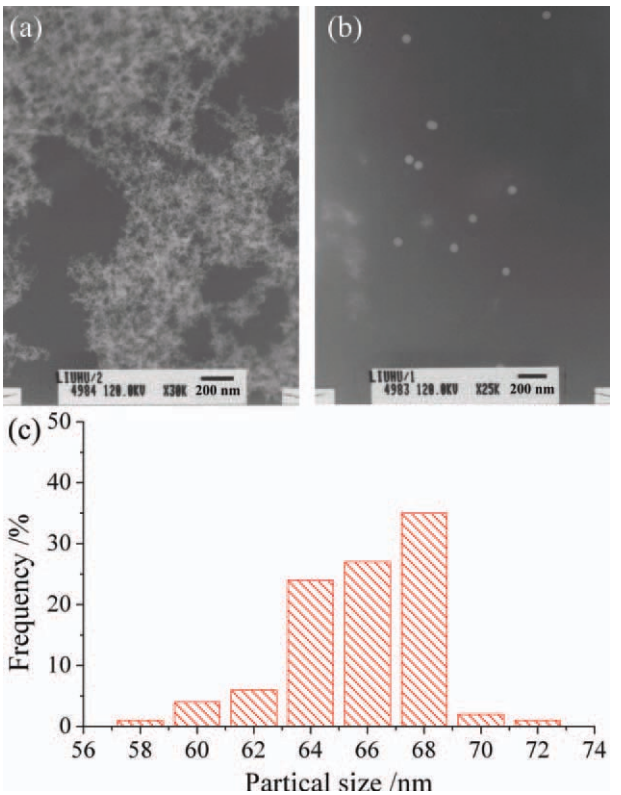

Figure 4. TEM images of $mSiO_2$ before (a) and after (b) *in situ* solution polymerization; (c) size distribution of $mSiO_2$ after *in situ* solution polymerization. [Color figure can be viewed in the online issue, which is available at wileyonlinelibrary.com.]

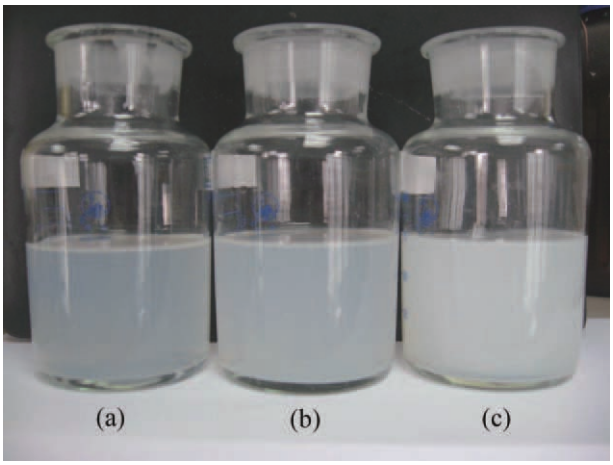

Figure 5. Optical picture of PHFA/$mSiO_2$ nanocomposite solutions with $mSiO_2$ of 0.5 wt % (a), 1.0 wt % (b) and 2.0 wt % (c) after standing for three months at room temperature.

Hong's result of 3.1%, suggesting a favorable modification method.[7]

Figure 3 showed the hydrophobic behavior of pure and modified nanosilicas in water. For the pure SiO_2, due to the abundant hydroxyl groups on the particles surface, the particles were hydrophilic and suspended well in water. On the contrary, $mSiO_2$ was hydrophobic and still floated on water even after violent stirring. The grafted C=C groups improved particles hydrophobicity and the compatibility of $mSiO_2$ in organic monomers and solvents. Furthermore, C=C groups can participate in polymerization with monomers, so the connection between inorganic particles and organic polymer could be build through chemical bonds.

Preparation of PHFA/$mSiO_2$ Nanocomposites

TEM images of dispersion state of $mSiO_2$ before and after *in situ* solution polymerization were displayed in Figure 4. As can be seen from Figure 4(a), nanosilicas aggregated together. By contrast, after *in situ* solution polymerization, $mSiO_2$ particles can be well dispersed in polymeric matrix as shown in Figure 4(b) (sample 4). The size distribution of particles shown in image (b) was about 64–68 nm. The possible procedures for nanoparticles dispersing in polymeric matrix through *in situ* solution polymerization may proceed as follows. Before the reaction occurred, the soft aggregates, composed of the primary nanoparticles, were absorbed by the monomers. During the polymerization, the monomers gradually infiltrated into the gaps and space between the aggregated nanosilicas, and then the monomer free radicals reacted with C=C groups on the surface of $mSiO_2$. The polymer chains grew at the particle surface and wrapped the particle. In this method, the gap between the particles was enlarged and consequently the aggregates disintegrated. Nanosilicas were eventually dispersed and kept in the resultant polymeric matrix through covalent bond.

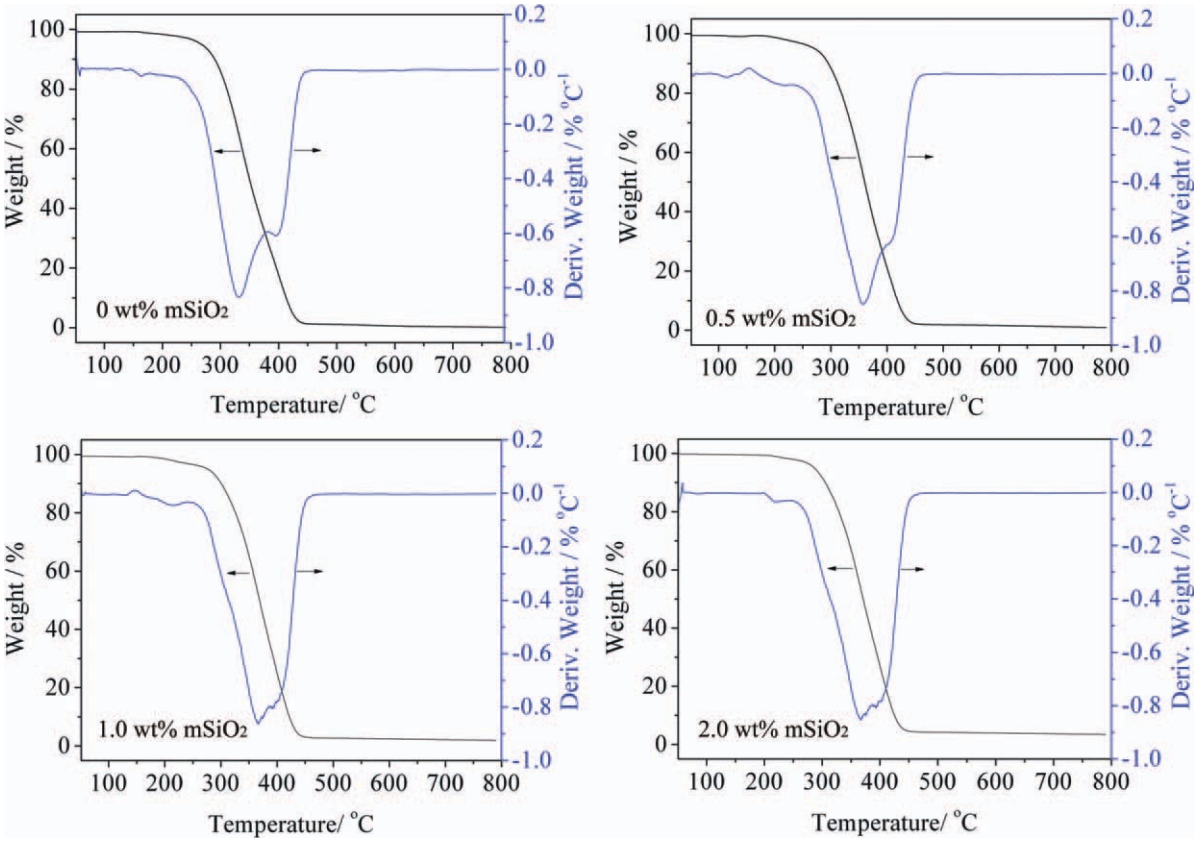

Figure 6. TG and DTG curves of PHFA/$mSiO_2$ nanocomposites with different $mSiO_2$ content. [Color figure can be viewed in the online issue, which is available at wileyonlinelibrary.com.]

Table II. TGA Results of PHFA/$mSiO_2$ Nanocomposites

Samples	$mSiO_2$ content (wt %)	$T_{d5\%}$[a] (°C)	$T_{d50\%}$[b] (°C)	T_{max}[c] (°C)
1	0	267.5	349.6	335.6
2	0.5	271.0	360.1	355.7
3	1.0	276.6	367.7	366.4
4	2.0	283.9	371.1	368.1

The results are the average value of two measurements for each sample. [a]The temperature at 5% weight loss, [b]The temperature at 50% weight loss, [c]The temperature at the maximum rate of weight loss, determined from the peak value in DTG curve.

Figure 5(a,b,c) displayed orderly the PHFA/$mSiO_2$ nanocomposite solutions with $mSiO_2$ content of 0.5, 1.0, and 2.0 wt % after standing for 3 months at room temperature (23°C ± 1°C). It was observed from Figure 5 that the solutions were milky white and no obvious phase separation to naked eyes, indicating that nanosilica particles suspended well in the polymeric matrix. To verify the effect of double bond on nanosilicas dispersion in polymer, a contrast experiment was performed. Dimethyldichlorosilance (DDS)-modified nanosilicas were chosen and employed in polymerization with the same procedure of synthesizing PHFA/$mSiO_2$ nanocomposites. The nanosilicas became hydrophobic after modification with DDS and suspended in the result polymer solution initially. However, compared with the above-mentioned nanocomposite solutions, a huge difference was observed for sample prepared by DDS-modified nanosilicas, which a thick layer of nanosilicas was settled at the bottom of the bottle within three days, implying that the suspension stability was poor. Due to the effect of Van der Waals force, DDS-modified silica particles could disperse in polymeric matrix initially. As compared with covalent bond, Van der Waals force was too weak to maintain the well dispersion, so the silica particles were precipitated under the influence of gravity. The results revealed that the improving of hydrophobicity of nanoparticles alone was not enough for preparation of a successful nanocomposite. Modification of the nanoparticles with reactive functional group and involvement of them in polymerization were another more essential factors. The C=C groups on the surface of $mSiO_2$ particles could react with the monomers and hence increase the interfacial strength between the nanoparticles and polymeric matrix.

Thermogravimetric Analysis of PHFA/$mSiO_2$ Nanocomposites

The thermal decomposition behavior of PHFA/$mSiO_2$ nanocomposites with different contents of $mSiO_2$ was investigated by TGA at a heating rate of 20°C min^{-1} under nitrogen flow. The curves of thermal gravimetry (TG) and differential thermal gravimetry (DTG) were obtained and illustrated in Figure 6. It was evident that all the PHFA/$mSiO_2$ nanocomposites had a higher onset decomposition temperature than pure PHFA. The peaks in DTG curves corresponded to the temperatures at maximum rate of weight loss (T_{max}). Table II represented the temperature data of 5% weight loss ($T_{d5\%}$), 50% weight loss ($T_{d50\%}$), and T_{max} for pure PHFA, and PHFA/$mSiO_2$ nanocomposites. Former researchers commonly considered $T_{d50\%}$ as an indicator for structural destabilization.[32] In this study, $T_{d50\%}$ for the pure PHFA, 0.5, 1.0, and 2.0 wt % PHFA/$mSiO_2$ nanocomposites were occurred at 349.6, 360.1, 367.7, and 371.1°C, respectively. $T_{d50\%}$ of the nanocomposite was enhanced by 21.5°C with the addition of 2.0 wt % $mSiO_2$. Also $T_{d5\%}$ and T_{max} gradually improved with the increase of $mSiO_2$ loading. Generally, polymer having higher crosslinking density showed higher decomposition temperature, and the crosslinking density increased with $mSiO_2$ loading content. In fact, the embedding nanosilicas in polymeric matrix played a role of anchor points, which can link the polymer chains together and restrict the motion of the polymer chains. The increment in decomposition temperature with $mSiO_2$ loading was also due to the barrier action to reduce the permeability of the heat current by ceramic nature of the nanosilica particles. This enhancing effect of nanosilica particles on thermal stability was also found in poly(ethylene 2,6-naphthalate)/silica nanocomposites and poly(propylene) layered silicate nanocomposites.[33,34]

Tensile Test of the Polyurethane Membranes

Figure 7 displayed the typical stress–strain behavior of the polyurethane membranes with different $mSiO_2$ loading amount. In comparison with neat polyurethane membrane, the composites showed prominent improvement of UTS and εB and the values increased with the addition of $mSiO_2$ content. From the linear portion of the curve, where Hook's law was valid, the values of Young's modulus were calculated for each sample. Table III summarized the results of UTS, εB, and E. The sample with 2.0 wt % of $mSiO_2$ gave the highest UTS (16.72 MPa), which was about 5.19 times higher than that of neat polyurethane material (3.22 MPa). As already discussed, this increase in tensile strength could be attributed to the strong interaction between the polymeric matrix and the silica particles resulting from the covalent bonds formed through *in situ* polymerization. Similar result was also obtained by Chen et al. in their study.[35] The improvement in mechanical properties is seen upon addition of silica nanoparticles, but this improvement could also be ascribed to some other possible factors, such as change in polymer morphology, crystallinity, which will be further studied in future.

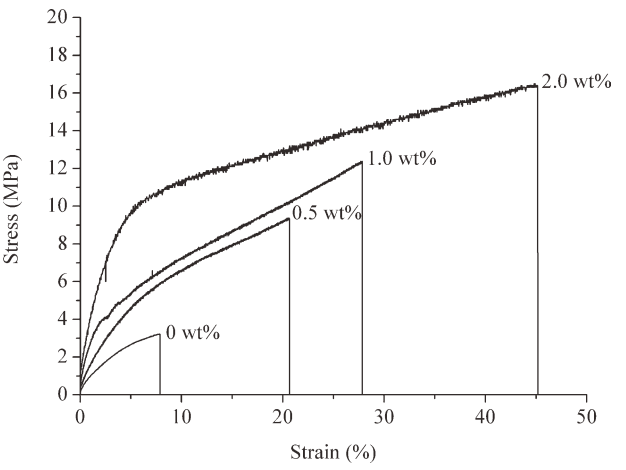

Figure 7. Typical stress–strain curves for polyurethane membranes with different $mSiO_2$ loading amount.

Table III. Tensile Properties of Polyurethane Membranes with Different $mSiO_2$ Content

Samples	$mSiO_2$ content (wt %)	Tensile properties		
		UTS (MPa)	εB (%)	E (MPa)
1	0	3.22 (0.24)[a]	7.8 (0.6)[a]	114.7 (12.6)[a]
2	0.5	9.31 (0.59)[b]	20.6 (1.3)[b]	139.5 (14.3)[b]
3	1.0	12.57 (0.89)[c]	27.9 (1.7)[c]	195.1 (19.5)[c]
4	2.0	16.72 (1.33)[d]	45.1 (3.6)[d]	312.4 (26.7)[d]

Entries were mean values with standard deviations in parentheses; any two means in the same column followed by the same superscript were not significantly different ($P > 0.05$).

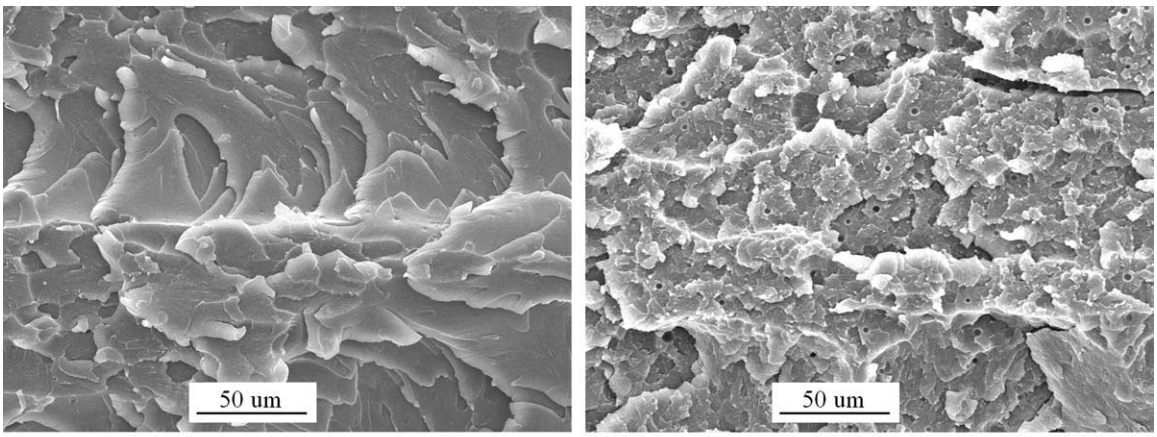

Figure 8. SEM images of the fractured surface of the snapped tensile test specimens (a) pure polyurethane material; (b) 2.0 wt % $mSiO_2$ composed.

Figure 8 showed the cross-section surfaces of the snapped tensile test samples. In the case of pure polyurethane material [Figure 8(a)], the fractured surface was very smooth and had uniform crack direction, which was indicative of brittle fracture and a weak resistance to crack propagation. As for polyurethane nanocomposites with 2.0 wt % of $mSiO_2$ content [Figure 8(b)], the fractured surface presented a rough and irregular appearance. According to reported literatures, the rigid particles in the polymeric matrix can bring out the effect of stress concentration, which can generate a large amount of "crazes."[36,37] During this process, the tensile energy was partially absorbed. Furthermore, due to the existence of rigid particles, crack extension in polymeric matrix was hindered and prevented to develop into destructive crack. In macroscopic view, it showed the characteristic of plastic fracture and the enhancement in tensile strength.

Surface Properties of the Polyurethane Films

The surface energy is also named surface free energy, which can be calculated in terms of contact angles of two kinds of liquids on the film surface. As larger the contact angle lower is the surface energy. Polymers with low surface energy are widely used in the areas of marine antifouling paints and antigraffiti coatings.[38,39] It is expected that the introduction of fluorinated groups in polymer can enhance the hydrophobicity of the film's surface. It is well known that fluorinated groups have the strong tendency to migrate toward interface and preferentially occupy the polymer–air interface to minimize the interfacial energy during the film-forming process.[17,40,41] As presented in Table IV, the water contact angles on each sample films are all above 90°, with surface energies less than 25 mN m^{-1}, which means that all the sample surfaces are hydrophobic.[42] In addition, one can see that $mSiO_2$ content has no obvious influence on surface

Table IV. Contact Angles and Surface Energies of Polyurethane Films with Different $mSiO_2$ Content

Samples	$mSiO_2$ content (wt %)	Contact angle (°)		Surface energy (mN m^{-1})		
		Water	Glycol	γ_s^d	γ_s^p	γ_s
1	0	96.8	71.4	22.90	1.86	24.76
2	0.5	98.7	73.1	23.08	1.40	24.48
3	1.0	97.5	72.0	23.01	1.68	24.69
4	2.0	98.2	72.7	22.96	1.53	24.49

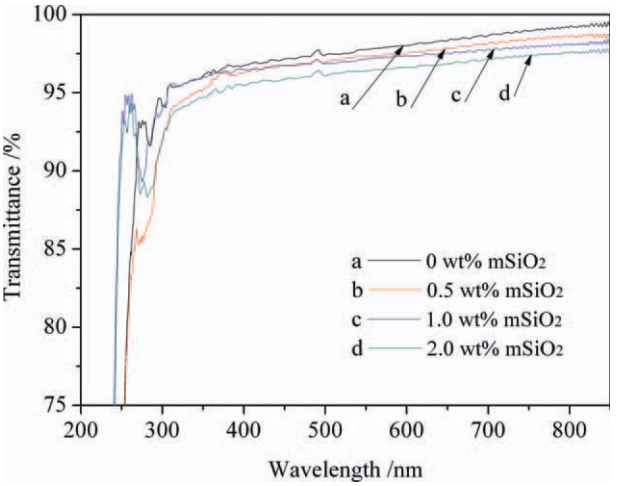

Figure 9. UV–vis transmission spectra of polyurethane films with different content of $mSiO_2$. [Color figure can be viewed in the online issue, which is available at wileyonlinelibrary.com.]

energy. Shafrin et al. have pointed out that the wettability of organic surfaces is determined by the nature and packing of the surface atoms or exposed groups of atoms of the solid and is otherwise independent of the nature and arrangements of the underlying atoms and molecules.[43] Therefore, the inside $mSiO_2$ particles cannot act on the surface energy. The dosages of fluorinated monomer (DFHMA) in each sample are the same, so the surface energies of the samples are nearly the same.

The Light Transmittance of the Polyurethane Films

The optical transparency of nanocomposites is also an important parameter for their practical applications such as optical fiber coating, lens coating, safety glass. The light transmittance of the polyurethane films with different amounts of $mSiO_2$ was recorded on Shimadzu 2450 UV–vis Spectrometer as shown in Figure 9. For pure polyurethane film, the light transmittance at the wavelength of 600 nm was as high as (98 ± 0.1)%. The transparency of the polyurethane films at visible light wavelength range (400–800 nm) was not affected significantly by the addition of $mSiO_2$ contents, and the transmittance at the wavelength of 600 nm still remained (96 ± 0.1)% for polyurethane film with 2.0 wt % of $mSiO_2$. Two necessities are required for high light transmittance; one is that the diameter of $mSiO_2$ nanoparticles should be less than the wavelength of visible light.[44] The other is uniformly dispersed nanoparticles in the matrix, which is also confirmed by Ou and Tan in their researches.[45,46] The application of the PHFA/$mSiO_2$ nanocomposite will be conducted in the following research.

CONCLUSIONS

In this article, poly(hydroxylic fluoroacrylate)/$mSiO_2$ nanocomposite was successfully prepared by *in situ* solution polymerization of monomers with vinyl groups modified SiO_2 ($mSiO_2$). Chemical bonds were formed between $mSiO_2$ and PFHA. TEM characterization showed a well dispersion of $mSiO_2$ nanoparticles in polymeric matrix after *in situ* solution polymerization. The introduction of $mSiO_2$ nanoparticles significantly improved the thermal stability and ultimate tensile strength of the resultant polymer, and the fracture behavior of the polyurethane membranes changed from as observed by SEM. The polyurethane films had low surface energy of lower than 25 mN m^{-1} and the light transmittance was not affected significantly by the addition of $mSiO_2$. According to the results, some promising applications of the synthesized nanocomposite may be suggested in the fields of transparent coating, antifouling paint, and anti-graffiti coating.

ACKNOWLEDGMENTS

The authors are grateful to the National Natural Science Foundation of China for financial support (Grant No. 21076044).

REFERENCES

1. Mishra, R. S.; Mishra, A. K.; Raju, K. V. S. N. *Eur. Polym. J.* **2009,** *45*, 960.
2. Zandi-zand, R.; Ershad-langroudi, A.; Rahimi, A. *Prog. Org. Coat.* **2005,** *53*, 286.
3. Zhang, C. H.; Zhang, Z. Q.; Li, Q. Y.; Cao, H. L. *Polym. Polym. Compos.* **2005,** *13*, 199.
4. Ma, J.; Mo, M. S.; Du, X. S.; Rosso, P.; Friedrich, K.; Kuan, H. C. *Polymer* **2008,** *49*, 3510.
5. Morgan, A. B.; Putthanarat, S. *Polym. Degrad. Stab.* **2011,** *96*, 23.
6. Yu, H. J.; Wang, L.; Shi, Q.; Jiang, G. H.; Zhao, Z. R.; Dong, X. C. *Prog. Org. Coat.* **2006,** *55*, 296.
7. Hong, R. Y.; Fu, H. P.; Zhang, Y. J.; Liu, L.; Wang, J.; Li, H. Z.; Zheng, Y. *J. Appl. Polym. Sci.* **2007,** *105*, 2176.
8. Zheng, J. P.; Zhu, R.; He, Z. H.; Cheng, G.; Wang, H. Y.; Yao, K. D. *J. Appl. Polym. Sci.* **2010,** *115*, 1975.
9. Cai, L. F.; Lin, Z. Y.; Qian, H. *Expr. Polym. Lett.* **2010,** *4*, 397.
10. Guo, Y. K.; Wang, M. Y.; Zhang, H. Q.; Liu, G. D.; Zhang, L. Q.; Qu, X. W. *J. Appl. Polym. Sci.* **2008,** *107*, 2671.
11. Liu, X. Y.; Zhao, H. P.; Li, L.; Yan, J.; Zha, L. S. *J. Macromol. Sci. Part A-Pure Appl. Chem.* **2006,** *43*, 1757.
12. Do, K. M.; Yuvaraj, H.; Woo, M. H.; Kim, H. G.; Jeong, E. D.; Johnston, K. P.; Lim, K. T. *Colloid Polym. Sci.* **2008,** *286*, 1343.
13. Luo, Z. H.; He, T. Y. *React. Funct. Polym.* **2008,** *68*, 931.
14. van Ravenstein, L.; Ming, W.; van de Grampel, R. D.; van der Linde, R.; de With, G.; Loontjens, T.; Thune, P. C.; Niemantsverdriet, J. W. *Macromolecules* **2004,** *37*, 408.
15. Kharitonov, A. P. *Prog. Org. Coat.* **2008,** *61*, 192.
16. Yarbrough, J. C.; Rolland, J. P.; DeSimone, J. M.; Callow, M. E.; Finlay, J. A.; Callow, J. A. *Macromolecules* **2006,** *39*, 2521.
17. Chen, L. J.; Shi, H. X.; Wu, H. K.; Xiang, J. P. *J. Fluorine Chem.* **2010,** *131*, 731.
18. Xiong, S. D.; Guo, X. L.; Li, L.; Wu, S. L.; Chu, P. K.; Xu, Z. S. *J. Fluorine Chem.* **2010,** *131*, 417.
19. Qu, A. L.; Wen, X. F.; Pi, P. H.; Cheng, J.; Yang, Z. R. *Polym. Int.* **2008,** *57*, 1287.

20. Qu, A.; Wen, X.; Pi, P.; Cheng, J.; Yang, Z. *J. Colloid Interface Sci.* **2008,** *317*, 62.
21. Liang, J. Y.; He, L.; Zheng, Y. S. *J. Appl. Polym. Sci.* **2009,** *112*, 1615.
22. He, L.; Liang, J. Y. *J. Fluorine Chem.* **2008,** *129*, 590.
23. Zhang, W.; Ni, H. G.; Wang, X. P. *Expr. Polym. Lett.* **2007,** *1*, 32.
24. Chen, Y. C.; Zhou, S. X.; Yang, H. H.; Wu, L. M. *J. Appl. Polym. Sci.* **2005,** *95*, 1032.
25. Stober, W.; Fink, A.; Bohn, E. *J. Colloid Interface Sci.* **1968,** *26*, 62.
26. Fowkes, F. M. *Indust. Eng. Chem.* **1964,** *56*, 40.
27. Owens, D. K.; Wendt, R. C. *J. Appl. Polym. Sci.* **1969,** *13*, 1741.
28. Song, W.; Gu, A. J.; Liang, G. Z.; Yuan, L. *Appl. Surf. Sci.* **2011,** *257*, 4069.
29. Duran, A.; Navarro, J. M. F.; Casariego, P.; Joglar, A. *J. Non-Cryst. Solids* **1986,** *82*, 391.
30. Chen, Y. J.; Cheng, S. Y.; Wang, Y. F.; Zhang, C. C. *J. Appl. Polym. Sci.* **2006,** *99*, 107.
31. Hong, R. Y.; Pan, T. T.; Qian, J. Z.; Li, H. Z. *Chem. Eng. J. (Lausanne)* **2006,** *119*, 71.
32. Mathew, A. P.; Packirisamy, S.; Thomas, S. *Polym. Degrad. Stab.* **2001,** *72*, 423.
33. Kim, J. Y.; Kim, D. K.; Kim, S. H. *Polym. Compos.* **2009,** *30*, 1779.
34. Zanetti, M.; Camino, G.; Reichert, P.; Mulhaupt, R. *Macromol. Rapid Commun.* **2001,** *22*, 176.
35. Chen, B. K.; Chiu, T. M.; Tsay, S. Y. *J. Appl. Polym. Sci.* **2004,** *94*, 382.
36. Shi, Q. A.; Wang, L.; Yu, H. J.; Jiang, S.; Zhao, Z. R.; Dong, X. C. *Macromol. Mater. Eng.* **2006,** *291*, 53.
37. Wazzan, A. A.; Al-Turaif, H. A.; Abdelkader, A. F. *Polym.-Plast. Technol. Eng.* **2006,** *45*, 1155.
38. Rath, S. K.; Chavan, J. G.; Sasane, S.; Jagannath; Patri, M.; Samui, A. B.; Chakraborty, B. C. *Appl. Surf. Sci.* **2010,** *256*, 2440.
39. Rabea, A. M.; Mohseni, M.; Mirabedini, S. M. *J. Coat. Technol. Res.* **2011,** *8*, 497.
40. Thomas, R. R.; Glaspey, D. F.; DuBois, D. C.; Kirchner, J. R.; Anton, D. R.; Lloyd, K. G.; Stika, K. M. *Langmuir* **2000,** *16*, 6898.
41. Cui, X. J.; Zhong, S. L.; Wang, H. Y. *Polymer* **2007,** *48*, 7241.
42. Gao, J. Z.; Wang, X. M.; Wei, Y. X.; Yang, W. *J. Fluorine Chem.* **2006,** *127*, 282.
43. Shafrin, E. G.; Zisman, W. A. *J. Phys. Chem.* **1960,** *64*, 519.
44. Chou, Y. C.; Wang, Y. Y.; Hsieh, T. E. *J. Appl. Polym. Sci.* **2007,** *105*, 2073.
45. Ou, C. F.; Shiu, M. C. *J. Appl. Polym. Sci.* **2010,** *115*, 2648.
46. Tan, H. L.; Yang, D. Z.; Xiao, M.; Han, J.; Nie, J. *J. Appl. Polym. Sci.* **2009,** *111*, 1936.